Int J Artif Organs 2011; 34 (5): 442-455 DOI: 10.5301/IJAO.2011.8361

ORIGINAL ARTICLE

PUCA pump and IABP comparison: analysis of hemodynamic and energetic effects using a digital computer model of the circulation

Libera Fresiello[1,2], Y. John Gu[3], Gianfranco Ferrari[1], Arianna Di Molfetta[1,4], Gerhard Rakhorst[3]

[1]Institute of Clinical Physiology, CNR, Rome - Italy
[2] Nałecz Institute of Biocybernetics and Biomedical Engineering, Polish Academy of Sciences, Warsaw - Poland
[3]Biomedical Engineering and Cardio-Thoracic Surgery, University Medical Center, Groningen - The Netherlands
[4]Tor Vergata University, Department of Cardiology, Rome - Italy

ABSTRACT

The pulsatile catheter pump (PUCA pump) is a left ventricular assist device that provides additional flow to the left ventricle. It is usually run in order to ensure a counterpulsation effect, as in the case of the intra-aortic balloon pump (IABP). Because of this similarity, a comparison between the PUCA pump and the IABP was conducted from both the hemodynamic and energetic points of view. Numerical models of the two devices were created and connected to the CARDIOSIM cardiovascular simulator. The PUCA and IABP models were then verified using in vivo experimental data and literature data, respectively. Numerical experiments were conducted for different values of left ventricular end systolic elastance (Els) and systemic arterial compliance (Csa). The energetic comparison was conducted taking into account the diastolic pressure time index and the endocardial viability ratio. Hemodynamic results expressed as cardiac output (CO) and mean coronary blood flow (CBF) show that both the IABP and the PUCA pump efficacy decrease with higher values of Els and Csa. The IABP especially shows higher sensitivity to these parameters, to the extent that in some cases CO actually drops and CBF does not increase. On the other hand, for lower values of Csa, IABP performance improves so much that the PUCA pump flow needs to be increased in order to ensure a hemodynamic effect comparable to that of the IABP. Energetic results show a trend similar to the hemodynamic ones. The study will be continued by investigating other energetic variables and the autonomic response of the cardiovascular system.

KEY WORDS: *IABP, PUCA pump, Cardiovascular system modeling, Counterpulsation effect, Left ventricular elastance, Lumped parameter model*

Accepted: February 17, 2011

INTRODUCTION

The pulsatile catheter pump (PUCA pump) and the intra-aortic balloon pump (IABP) are both devices intended to support impaired ventricular function and assist heart recovery in cardiogenic shock, acute myocardial infarction, and other heart conditions characterized by a low output failure (1, 2).

The pulsatile catheter pump (PUCA pump) consists of a hydraulically or pneumatically driven membrane pump connected to a valved catheter. It is positioned with the tip into the left ventricle while an inflow valve permits blood to be aspirated from the ventricle. A second valve then ensures the ejection of blood into the ascending aorta (1).

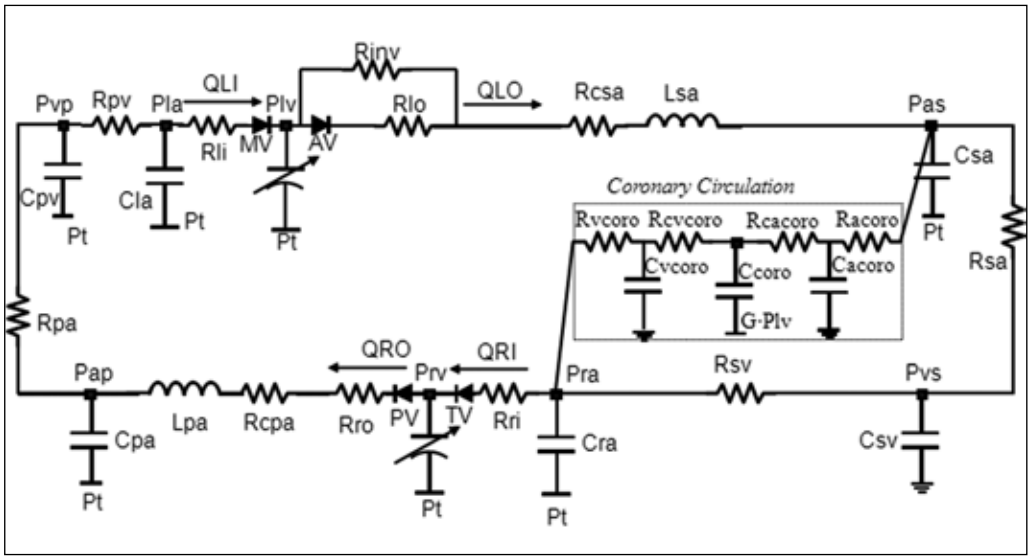

Fig. 1 - *Electric analogue of the cardiovascular system numerical model.*

One of the main advantages of the PUCA pump is that it can be introduced through an easily accessible artery, thus helping to reduce surgical trauma (3).

The PUCA pump can be ECG-triggered with or without a delay after the ventricular systole or, in the case of a patient with severe arrhythmia, it can be switched to asynchronous functioning. It is also possible to set different synchronization ratios between the PUCA pump frequency and the heart rate. Indeed, beyond a certain heart rate, a synchronization ratio of 1:2 or 1:3 is preferred, thus causing the PUCA pump to eject blood each second or third cardiac cycle and making the filling time long enough to ensure the device performs well (4). Considering that the pump is usually synchronized in counterpulsation modality and that it pumps blood from the left ventricle into the aorta, the two main expected effects are: an unloading of the left ventricle and an improvement of the coronary blood flow (5). These effects are quite similar to those of the intra-aortic balloon pump (IABP). The IABP provides a counterpulsation action through the inflation and deflation of a balloon into the descending aorta, thus improving the coronary blood flow and the left ventricular oxygen supply (6).

In spite of these similarities, the two devices have a different mechanical action and a comparison between them can be helpful to analyze their sensitivity to specific ventricular and circulatory parameters. Naturally, the two devices should be compared under the same hemodynamic conditions, a hard task for *in vivo* experiments which are characterized by intrinsic randomness. As a partial solution to this problem, comprehensive models of the cardiocirculatory system can be used (7-11). Numerical models have the advantage of being flexible and guaranteeing the repeatability of each experiment. Moreover, they enable the sensitivity of the combined system (cardiovascular system plus mechanical circulatory support system) to be differentiated in response to each hemodynamic parameter change, one by one. The aim of this work was therefore to perform a comparison between the PUCA pump and the IABP in terms of hemodynamics and energy. To conduct this study, a previously developed circulatory model (12) was connected to a numerical model of the PUCA pump and of the IABP, respectively.

MATERIALS AND METHODS

The cardiovascular model

CARDIOSIM software is a numerical simulator of the cardiovascular system that reproduces main hemodynamic phenomena in terms of pressures and flows. Each circulatory district was schematized by a lumped parameter model as shown in Figure 1. Nomenclature is reported in Table I.

Atria are passive and were represented by single compliances. For both ventricles, a time-varying elastance model was used for the representation of the ejection phase, and a sum of exponential functions for the representation of the filling phase (12-14).

TABLE I - ABBREVIATIONS USED IN FIGURE 1

Parameter	Symbol	Unit
Left (right) heart		
Rli (Rlo)	Left input (output) valve resistance	[g cm^{-4} s^{-1}]
Rri (Rro)	Right input (output) valve resistance	[g cm^{-4} s^{-1}]
Pla (Pra)	Left (right) atrial pressure	[mmHg]
Plv (Prv)	Left (right) ventricular pressure	[mmHg]
QLI (QLO)	Left ventricular input (output) flow	[l min^{-1}]
QRI (QRO)	Right ventricular input (output) flow	[l min^{-1}]
MV (TV)	Mitral valve (Tricuspid valve)	
AV (PV)	Aortic valve (Pulmonary valve)	
Rinv	Aortic valve inverse resistance	[g cm^{-4} s^{-1}]
V_{0LV} (V_{0RV})	Theoretical left (right) ventricular volume at zero pressure	[cm^3]
Els (Ers)	End systolic left (right) ventricular elastance	mmHg cm^{-3}
Cla (Cra)	Left (right) atrial compliance	[cm^3 $mmHg^{-1}$]
Systemic (Pulmonary) Arterial Section		
Rcsa (Rcpa)	Systemic (pulmonary) characteristic resistance	[g cm^{-4} s^{-1}]
Lsa (Lpa)	Systemic (pulmonary) inertance	[mmHg cm^{-3} sec^2]
Csa (Cpa)	Systemic (pulmonary) arterial compliance	[cm^3 $mmHg^{-1}$]
Lsa (Lpa)	Systemic (pulmonary) inertance	[mmHg $cm^{-3}sec^2$]
Csa (Cpa)	Systemic (pulmonary) arterial compliance	[cm^3 $mmHg^{-1}$]
Systemic (Pulmonary) Venous Section		
Rsv (Rpv)	Systemic (Pulmonary) resistance	[g cm^{-4} s^{-1}]
Csv (Cpv)	Systemic (Pulmonary) venous compliance	[cm^3 $mmHg^{-1}$]
Pvs (Pvp)	Systemic (Pulmonary) venous pressure	[mmHg]
Coronary Section		
Racoro	Resistance of coronary arteries	[g cm^{-4} s^{-1}]
Rvcoro	Resistance of coronary veins	[g cm^{-4} s^{-1}]
Rcacoro	Arterial capillary resistance	[g cm^{-4} s^{-1}]
Rcvcoro	Venous capillary resistance	[g cm^{-4} s^{-1}]
Ccoro	Intramyocardial compliance	[cm^3 $mmHg^{-1}$]
Cacoro	Arterial coronary compliance	[cm^3 $mmHg^{-1}$]
Cvcoro	Venous coronary compliance	[cm^3 $mmHg^{-1}$]
CBF	Mean coronary blood flow	[cm^3 min^{-1}]
Pt	Intrathoracic pressure	[mmHg]
HR	Heart rate	[bpm]
CO	Cardiac output	[l min^{-1}]

The coronary circulation was described by an RC model (15, 16) shown in Figure 1. The model was connected with the cardiovascular system through the systemic arterial compliance (Csa) and the right atrial compliance (Cra). Intramyocardial compliance (Ccoro) was polarized by intramyocardial pressure (G·Plv), which was related to the left ventricular pressure by the constant G. A signal corresponding to the beginning of ventricular ejection is generated in the model and can play the role of the ECG being used as a reference to synchronize the PUCA pump and IABP.

The PUCA pump model

The numerical model of the PUCA pump, derived from a previous study (1), is able to reproduce the pressure drop between the catheter tip and the membrane pump according to:

$$P_{drive} - P_1 = \rho a L + \frac{1}{2}\rho v^2 \left(\frac{\lambda L}{d} + K_v + K_c \right) \quad \text{(Eq.) (1)}$$

where P_{drive} is the aspiration (ejection) pressure of the device; P_1 is the left ventricular (systemic arterial) pressure; ρ is the blood density (1.060 g cm^3); *L* and *d* are catheter length (40 cm) and diameter (we chose 21 Fr and 25 Fr), respectively; while *a* and *v* are the acceleration and the velocity of the blood in the catheter, respectively. K_c is the resistance due to diameter change between the membrane and the catheter, and K_v is the resistance due to the inflow and outflow valves (Fig. 2). As the blood flowing in the catheter is assumed to be turbulent (Reynolds' number >4.000) a resistance factor was introduced (1):

$$\lambda = 0.096 - \left[0.0157 \times \log_{10}(Re) \right] \quad \text{(Eq.) (2)}$$

Blood is presumed to be Newtonian, with a dynamic viscosity μ of 0.0036 Pa s. The numerical model is also able to synchronize the PUCA pump as it was discussed in the introduction. A more detailed description of the numerical model and of its interaction with the cardiovascular system is reported in (17).

The IABP model

According to Jaron et al (2, 18), the IABP is considered as a flow source because the rate of change of balloon volume is equal to the rate of change of blood displaced in the aorta. In particular, during diastole the balloon inflation provides a flow from the aorta towards the ventricle, while during systole the balloon deflation provides a flow in the opposite direction. The flow source can be replaced by a pressure source $P_{iabp}(t)$ describing the compressed air reservoir and by a resistance R_{iabp} of 667 g·cm^{-4} s^{-1} describing the equivalent resistance of the gas delivery system (18). In the case of incompressible gas, volume change in the balloon (V_{iabp}) is related to the gas flow rate in the catheter (Q_{cat}) just outside the balloon as follows:

$$\frac{dV_{iabp}}{dt} = Q_{cat} = \frac{P_{iabp} - Pas}{R_{iabp}} \quad \text{(Eq.) (3)}$$

The maximum volume considered for the balloon is 40 cm^3. The $P_{iabp}(t)$ is connected to a high pressure tank and a vacuum pressure tank alternately, able to fill and empty the balloon according to the signal generated by the cardiovascular numerical model. Balloon filling and emptying sync times are calculated from the beginning of the cardiac cycle. A more detailed description is reported in (2, 12, 18-20).

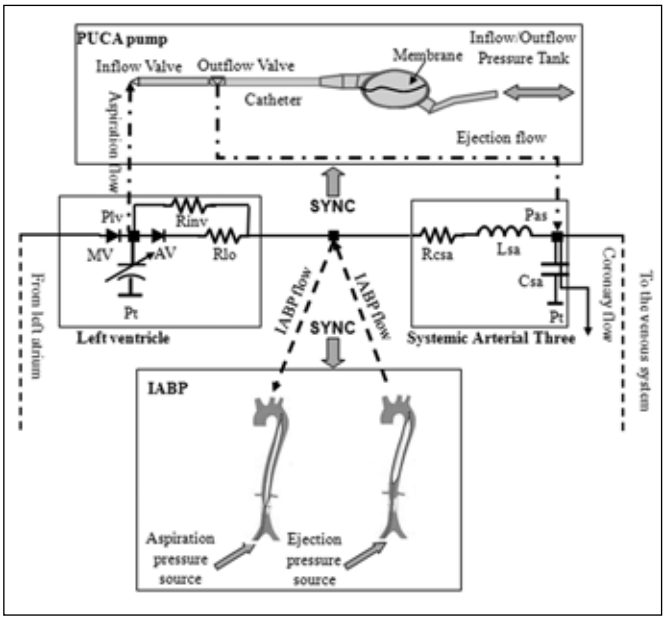

Fig. 2 - *Schematization of PUCA pump and IABP. They can be connected, one at a time, to the same cardiovascular simulator. A signal corresponding to the beginning of ventricular ejection is generated within the model (SYNC) and can play the role of the ECG being used as a reference to synchronize PUCA pump and IABP.*

PUCA pump numerical model verification

Experimental data collection

The system, comprising a PUCA pump and the cardiovascular simulator, was configured based on *in vivo* data collected from two pigs. Experimental data were used to configure the model and verify the hypotheses tested for simulations. Experiments were performed according to the rules of the ethical committee on animal research at the University Medical Center Groningen, The Netherlands. Pigs with a body weight of 70 kg and 76 kg were prohibited from any food for at least 8 h before operation. Anesthesia was induced with intramuscular injection of ketamine and diazepam followed by continuous inhalation of 2% isoflurane with 100% oxygen. During experiments, a triple-lumen Swan-Ganz catheter was inserted via the jugular vein towards the pulmonary artery to measure the central venous pressure, right ventricular pressure, and pulmonary arterial pressure. Then the carotid artery was set free and a cannula was inserted towards the ascending aorta to measure the mean arterial pressure. Afterwards, the chest was opened with a median sternotomy. A double-lumen Swan-Ganz catheter was positioned via the left auricle into the left ventricle to measure the left atrial pressure and left ventricular pressure. Heart rate was recorded by an electrocardiogram and cardiac output was determined by the thermodilution technique with a pulmonary artery catheter (Vigilance; Edwards Lifesciences, Irvine, CA, USA). Experiments were divided into three steps. After a basal measurement, the PUCA pump catheter (connected to a membrane pump) was inserted into the left ventricle through the ascending aorta. After a period of animal stabilization of 5 min, a second set of hemodynamic data was recorded. Then the PUCA pump was activated by an IABP driver and continued for 5 minutes prior to data recording. We analyzed two acquisitions for each experimental step.

To resume, for each animal, experimental data comprised the hemodynamic condition before PUCA pump insertion, after PUCA pump positioning (but not yet running) and after PUCA pump activation. The first experimental data set was used as control to analyze the PUCA pump working conditions. The remaining experimental data sets were used to define PUCA pump simulation parameters.

Simulation of PUCA pump working conditions

According to a previous study (3) a transvalvular device such as the PUCA pump may cause an aortic regurgitation. For this reason we carefully analyzed experimental data starting from acquisitions before PUCA pump insertion. Attention was focused on the analysis of the systemic arterial pressure (Pas) decay during diastole. It can be approximated by an exponential function:

$$Pas = Pas_0 \times \exp^{-\frac{t}{R_{tot} \times Csa}} \qquad \text{(Eq.) (4)}$$

where Pas_0 is the pressure at the beginning of the diastole; t is the time; and R_{tot} is the total arterial resistance that causes the discharge of the Csa. Using an experimental Pas decay waveform, before catheter insertion, the product $R_{tot} \cdot Csa$ can be estimated. If no aortic regurgitation occurs, the R_{tot} is coincident with the systemic arterial resistance Rsa, which can be calculated using the following equation:

$$Rsa = \frac{Pas - Pvs}{CO} \qquad \text{(Eq.) (5)}$$

where Pvs is the mean systemic venous pressure, and CO is the cardiac output.

Using Eqs. (4) and (5) together, it is possible to calculate the value of Csa before catheter insertion. The same value of Csa was used before and after catheter insertion since the variation in mean Pas was not particularly significant (less than 8 mmHg) (21).

As a second step, Eq. (4) was used also to analyze experimental Pas decay after PUCA pump insertion (but not yet running). Using the previously calculated Csa value, and considering the Pas decay waveform, it is possible to obtain a new R_{tot} value. From Eq. (5), then, the new value of Rsa after PUCA insertion was calculated as well. An Rsa value higher than R_{tot} indicates that Csa discharges on a resistance lower than the Rsa estimated using Eq. (5).

The aortic regurgitation can be schematized by a resistance R_{inv} (Fig. 1) able to reproduce a blood back-flow from the aorta into the left ventricle during diastole. As a first approximation, the R_{tot} can be expressed as:

$$\frac{1}{R_{tot}} = \frac{1}{Rsa} + \frac{1}{Rcsa + Rinv} \qquad \text{(Eq.) (6)}$$

where R_{csa} is the systemic characteristic resistance of the arterial section.

From this equation, the value of R_{inv}, in the case of aortic regurgitation ($R_{tot}<R_{sa}$), can be estimated. To calculate Rinv it was assumed that diastolic P_{lv} ~ average P_{vs}.
This procedure was used for each experiment in order to evaluate the presence of an aortic regurgitation and estimate Rinv if necessary. The other cardiovascular parameters of the animal, once the catheter is inserted but is not yet running, were estimated as indicated in Table II (second column).
As the final step, experimental data after PUCA pump activation were considered and the new consequent hemodynamic conditions were characterized and reproduced numerically, following the procedure described in Table II (third column).
The method described so far was used to reproduce numerically the hemodynamic conditions of all experiments (two for each animal) both before and after PUCA pump activation.

Comparison between experimental and simulation PUCA pump data

The difference between experimental and simulated data was evaluated by the percentage error (Eij). Eij was calculated for each experiment and each hemodynamic variable. Then, the Eij of the 4 experiments were used to calculate the average of the percentage error (Emj, Esdj) as follows:

$$Eij = 100 \times \frac{(Xij_{NM} - Xij_{EXP})}{Xij_{EXP}}$$
$$Emj = \frac{\sum_{4}^{i=1} abs(Eij)}{4} \quad \text{(Eq.) (7)}$$

Xij_{NM} is the mean value of the hemodynamic variable j, relative to the experiment i-th, obtained from the numerical model. Xij_{EXP} is the mean value of the hemodynamic variable j, relative to the experiment i-th, obtained from experimental data. This analysis was performed for both conditions before and after PUCA pump activation. The analyzed hemodynamic variables were: mean Pas, Pap, Pvs, Pla, CO, QLO, and QPUCA.

IABP numerical model verification

The verification of the IABP numerical model and of its interaction with the cardiovascular system was based on *in vivo* clinical data taken from the literature (22). Results concern both hemodynamic conditions before and straight after IABP activation. In this case as well a comparison

TABLE II - ESTIMATION OF HEMODYNAMIC PARAMETERS BEFORE AND AFTER PUCA PUMP ACTIVATION

Variables	Before PUCA pump activation	After PUCA pump activation
HR	HR_1 was estimated from experimental data before PUCA activation	HR_2 was estimated from experimental data after PUCA activation
V_{0LV}	A value of 25 cm^3 was chosen for all experiments	Unchanged
Rsa	Rsa_1 was estimated according to eq. 5 considering experimental data before PUCA activation	Rsa_2 was estimated according to eq. 5 considering experimental data after PUCA activation
Csa	Csa was estimated according to eq. 4 considering experimental data before PUCA insertion	Unchanged
Rinv	Rinv was estimated according to eq. 6 considering experimental data before PUCA activation	Unchanged
Els	Els value was set in order to reproduce experimental CO value before PUCA activation	Unchanged
Mean PUCA pump flow (QPUCA)	-	Obtained from experimental data after PUCA activation
PUCA pump temporization	-	Estimated on the basis of experimental PUCA flow waveforms after PUCA activation

was performed between simulated data and data from the literature. As the literature data already referred to the average hemodynamic conditions of 15 patients (both before and after IABP activation), a percentage error Ej was calculated as follows:

$$Ej = 100 \times \frac{(Xj_{NM} - Xmj_{LIT})}{Xmj_{LIT}} \quad \text{(Eq.) (8)}$$

where Xmj_{LIT} is the mean value of the hemodynamic variable j taken from (22), and Xj_{NM} is the mean value of the hemodynamic variable j, obtained from the numerical simulation.

PUCA pump and IABP comparison

The comparison between the PUCA pump and the IABP was performed under the same hemodynamic conditions. To this aim, the hemodynamic situation of one of the animals was chosen as the initial conditions in order to test the performance of both devices. Comparison between the two devices was performed basing on two considerations:

– clinical experience showed that IABP effects are smaller for higher values of Els whereas the PUCA pump improves hemodynamic conditions in these cases as well (3, 23).
– the counterpulsation effect is strongly influenced by the stiffness of the vascular system (24).

Therefore, after the reproduction of the initial hemodynamic conditions, ventricular (Els) and circulatory (Csa) parameters were changed, performing the simulations for both the IABP and the PUCA pump (Tab. III). In the case of the PUCA pump, additional simulations were performed changing QPUCA and catheter diameter to understand if a higher aspiration of blood from the left ventricle could ensure better PUCA pump performance (P5 in Tab. III).

The temporization of the PUCA pump was set according to experimental data (counterpulsation modality) for all experiments. For IABP simulations, the temporization was set to maximize both CO and CBF.

For both groups of experiments, CO and CBF were the hemodynamic variables used for comparison. Besides, as this work was also aimed at analyzing the energetic effects of the devices, a specific analysis of the tension time index (TTI) and the diastolic pressure time index (DPTI) was performed. TTI and DPTI provide information about the oxygen demand and supply to the myocardium, respectively (25).

TTI and DPTI were calculated as follows:

$$TTI = \int_{systole} Plv \times dt \quad \text{(Eq.) (9)}$$

$$DPTI = \int_{diastole} (Pas - Plv) \times dt \quad \text{(Eq.) (10)}$$

Their ratio is the endocardial viability ratio (EVR), an important index for the evaluation of the IABP counterpulsation performance (26):

$$EVR = DPTI / TTI \quad \text{(Eq.) (11)}$$

These variables are commonly used to evaluate IABP performance but in this work their use was also extended to the PUCA pump, as it is usually run in order to assure a counterpulsation effect.

TABLE III - CHARACTERIZATION OF NUMERICAL EXPERIMENTS USED FOR THE COMPARISON BETWEEN PUCA PUMP AND IABP

Numerical Experiments	IABP		PUCA pump				
Experiment symbol	I1	I2	P1	P2	P3	P4	P5
Els [mmHg cm^{-3}]	0.65 – 1.0 – 1.35 – 1.7						
Csa [cm^3 mmHg^{-1}]	3.3	1.0	3.3	3.3	1.0	1.0	1.0
Catheter d [Fr]	-	-	21	21	21	21	**25**
QPUCA [l min]	-	-	**2.9**	**3.4**	**3.0**	**3.7**	**5.0**
Rinv [g cm^{-4} s^{-1}]	Rinv=∞		1738	1738	1738	1738	1738

Parameters values used for all experiments: Rsa 958 g cm^{-4} s^{-1}, Rsca 29 g cm^{-4} s^{-1}, Csv 82.5 cm^3 mmHg^{-1}, Rap 135 g cm^{-4} s^{-1}, Rsv 7 g cm^{-4} s^{-1}, V_{0LV} 25 cm^3 , V_{0RV} 5 cm^3 HR 97 bpm.
Variables correspond to the hemodynamic conditions of one of the 4 experiments used for collecting in vivo data. "Experiment symbol" specifies the abbreviations used in the text to identify each numerical experiment.

RESULTS

Results are resumed in Figures 3, 4, and 5 and in Tables IV, V, and VI. The first part of this work was focused on the reproduction of the working conditions of the PUCA pump according to the experimental data. To this aim, the hemodynamic conditions of each experiment were characterized in terms of cardiovascular parameters according to the procedure indicated in Table II. All results are summarized in Table IV. As an example, in Figure 3 the comparison between simulated and experimental Pas and Plv waveforms is shown for one of the 4 experiments after characterization of the parameters.

The accuracy of numerical simulations was tested consid-

TABLE IV - PARAMETER VALUES OF THE HEMODYNAMIC CONDITIONS OF THE FOUR EXPERIMENTS

Animal	Exp	HR_1 [bpm]	Rsa_1 [g cm^{-4} s^{-1}]	HR_2 [bpm]	Rsa_2 [g cm^{-4} s^{-1}]	Rinv [g cm^{-4} s^{-1}]	Els [mmHg cm^{-3}]	Csa [cm^3 mmHg^{-1}]	V_{0LV} [cm^3]
1	1	97	951	114	859	1080	0.85	3.72	25
1	2	138	927	138	801	325	0.85	3.72	25
2	3	86	562	85	686	∞	1.35	3.30	25
2	4	95	707	97	958	1738	1.35	3.30	25
Average		104	787	109	826	1048	1.10	3.51	25
SD		±23	±186	±23	±114	±707	±0.29	±0.24	±0

Subscript 1 and 2 refer to hemodynamic values before and after PUCA pump activation. For Rinv both Average and Standard Deviation (SD) were calculated considering only Experiments 1-2-4.

TABLE V - PUCA PUMP: COMPARISON BETWEEN EXPERIMENTAL AND SIMULATED DATA

Before PUCA	Pas [mmHg]	Pvs [mmHg]	Pla [mmHg]	Pap [mmHg]	CO [l min]	QLO [l min]	QPUCA [l min]
Exp1	57.4	7.1	10.3	15.9	4.23	-	-
Sim1	59.2	7.0	10.6	16.8	4.39	-	-
Exp2	62.0	6.6	10.3	18.0	4.77	-	-
Sim2	57.7	6.9	11.1	18.9	4.70	-	-
Exp3	54.7	4.1	7.2	13.5	7.20	-	-
Sim3	54.6	4.2	7.6	14.0	6.93	-	-
Exp4	55.2	2.6	4.6	12.3	5.95	-	-
Sim4	57.8	2.8	4.6	12.7	6.10	-	-
After PUCA							
Exp1	59.4	7.0	10.0	15.9	4.89	2.34	2.55
Sim1	60.0	7.5	8.5	14.7	4.93	2.56	2.36
Exp2	59.1	6.6	10.2	17.8	5.24	2.99	2.25
Sim2	56.5	7.2	9.9	17.3	4.94	2.87	2.06
Exp3	65.0	3.8	7.0	14.5	7.13	4.23	2.90
Sim3	61.7	4.0	6.9	14.1	6.70	3.93	2.76
Exp4	64.4	2.6	4.7	13.4	5.16	2.46	2.70
Sim4	67.9	2.5	4.0	13.6	5.55	2.64	2.90
Mean Percentage Error							
	E_{mPas}	E_{mPvs}	E_{mPla}	E_{mPap}	E_{mCO}	E_{mQLO}	E_{mQPUCA}
Before PUCA	3.64	4.04	3.97	4.27	1.06	-	-
After PUCA	3.94	6.89	8.64	3.69	5.06	7.01	7.03

Upper rows: Mean values of pressures and flows before and after PUCA pump activation. Expi refers to i-th experimental values and Simi refers to values of the i-th numerical simulation. Lower rows: average of percentage error (Emij) between experimental and simulated data before and after PUCA pump activation. Before PUCA pump activation QPUCA=0 while after PUCA pump activation CO=QPUCA+QLO (with QLO left ventricular flow).

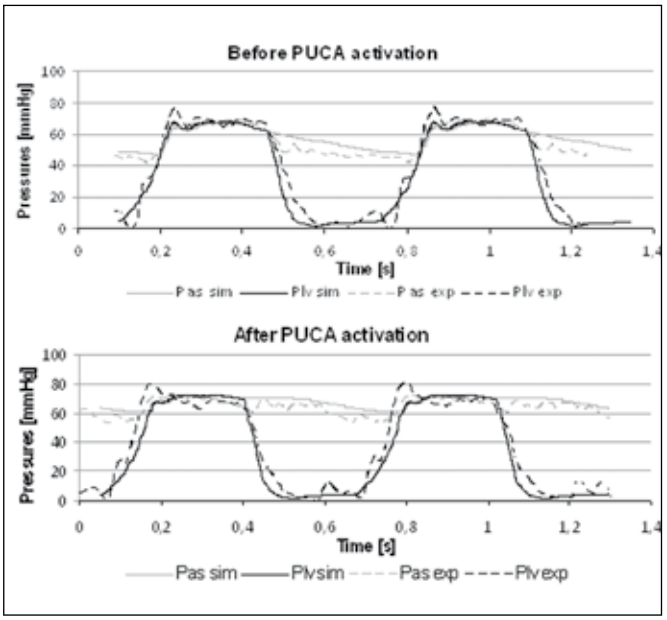

Fig. 3 - *Left ventricular (Plv) and systemic arterial (Pas) pressure waveforms: the upper figure refers to the comparison between experimental data (Pas exp and Plv exp) and simulated data (Pas sim and Plv sim) before PUCA pump activation; the lower figure refers to the comparison between experimental data and simulated data after PUCA pump activation.*

ering the average of the percentage errors calculated as indicated in Eq. (7). Table V shows good agreement between numerical simulations before PUCA pump activation and the corresponding experimental data. In fact, the percentage errors are less than 10% for each hemodynamic variable, with the sole exception of Pla. After PUCA pump activation, the percentage errors remain in the same range.

A similar evaluation for the IABP simulation was realized using literature data (22) referring to the average hemodynamic conditions of 15 patients before and after IABP activation. In this case percentage error Ej was calculated using Eq. (8). Table VI shows that for IABP as well, simulated variables differ from the literature data by less than 10%.

After verification of the PUCA and IABP models, the next step was the comparison between the PUCA pump and the IABP. As explained above, the comparison analysis was feasible because both devices were implemented on the same cardiovascular simulator. The study was conducted, in fact, by starting from the same hemodynamic situation (corresponding to Exp. 4 in Tab. IV) and then connecting the PUCA pump or the IABP model to the cardiovascular simulator. Each group of simulations, resumed in Table III (I1-P1-P2 and I2-P3-P4, P5), is therefore characterized by the same hemodynamic parameters with the only exception of Rinv. In the case of the IABP, the balloon is positioned in the descending aorta and no aortic regurgitation was simulated.

The effects of the PUCA pump and the IABP were assessed by evaluating the percentage variations of hemodynamic/energetic variables before and after device activation. In Figure 4, IABP and PUCA pump effects of experiments I1-P1-P2 in terms of CO and CBF (a-b) and in terms of energetic variables DPTI and EVR (c-d) are compared.

In the second part of the comparison analysis, the effects of both devices were analyzed in the case of a stiffer arterial system (experiments I2-P3-P4-P5 in Fig. 5). Also in this case the comparison analysis was performed

TABLE VI - IABP COMPARISON BETWEEN EXPERIMENTAL AND SIMULATED DATA

IABP	HR [bpm]	EDV [cm^3]	ESV [cm^3]	EDP [mmHg]	ESP [mmHg]	Pas [mmHg]	SV [cm^3]
Literature value before IABP (22)	76	272	212	11.3	92	71	53.3
Literature value after IABP (22)	76	266	199	9.7	76	82	60.5
Simulation value before IABP	76	264	209	10.5	85	73.8	55.3
Simulation value after IABP	76	260	201	9.0	80	77.8	58.9
Percentage error	E_{HR}	E_{EDV}	E_{ESV}	E_{EDP}	E_{ESP}	E_{Pas}	E_{SV}
Before IABP	0	-2.9	-1.5	-7.1	-7.6	3.9	3.8
After IABP	0	-2.2	1.2	-7.2	5.3	-5.1	-2.6

Upper rows: literature and simulated data of the IABP assistance. These data were used to calculate the percentage error Ej indicated in the last rows of the table. EDV is the end-diastolic left ventricular volume, ESV is the end-systolic left ventricular volume, ESP is the end systolic Pas, ESP is the end systolic Pas, SV is the stroke volume.

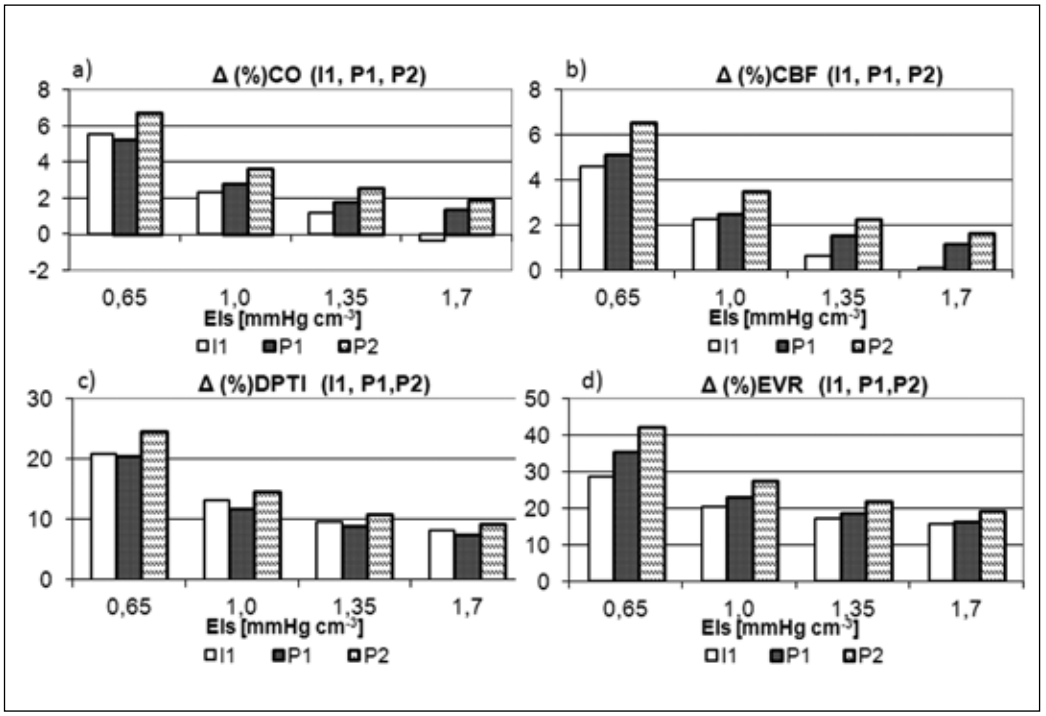

Fig. 4 - *Comparison between I1, P1 and P2 experiments: percentage variation of **(a)** CO, **(b)** CBF, **(c)** DPTI , and **(d)** EVR due to PUCA/IABP activation for different values of Els.*

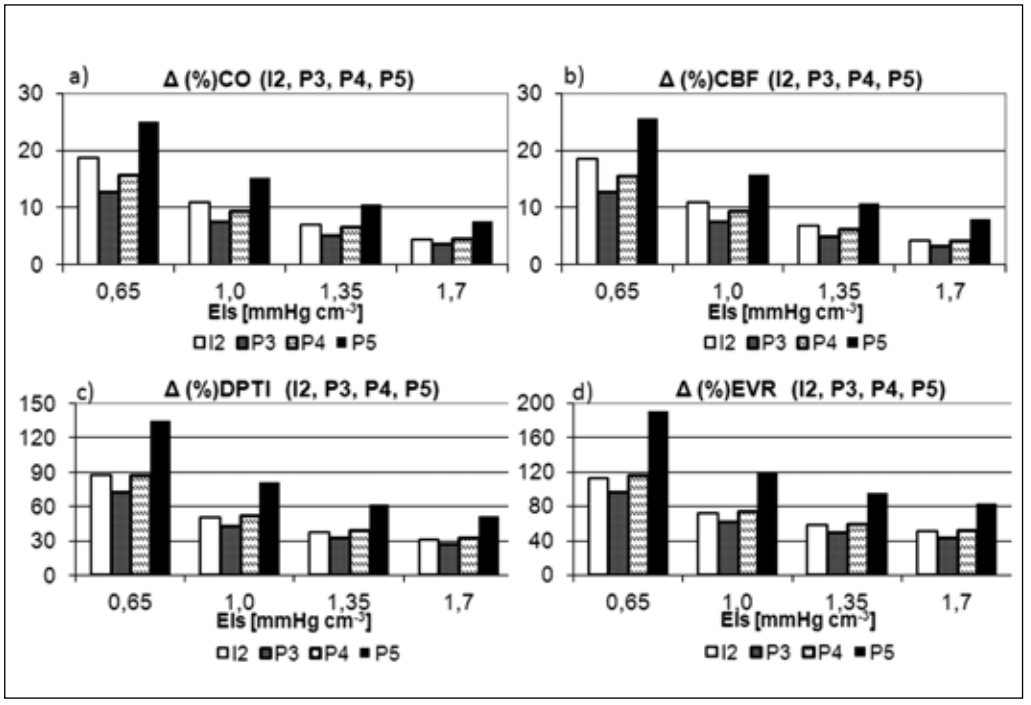

Fig. 5 - *Comparison between I2, P3, P4 and P5 experiments: percentage variation of **(a)** CO, **(b)** CBF, **(c)** DPTI , and **(d)** EVR due to PUCA/IABP activation for different values of Els.*

in terms of percentage variation of hemodynamic and energetic variables before and after devices onset. In particular, in Figure 5a and b, CBF and CO percentage variations are shown, while Figures 5c and d refer to the corresponding percentage variations of DPTI and EVR.

DISCUSSION

Results show that both numerical models can reproduce the behavior of the PUCA pump and the IABP with good accuracy (percentage errors <10%).

Comparison results, shown in Figures 4 and 5, were obtained simulating the hemodynamic conditions of one of the 4 experiments used for collecting *in vivo* data (Exp. 4 in Tab. IV). Experiment 4 was chosen in order to consider a higher Rinv value. From Table IV it is evident that Rinv is a critical parameter. In fact, not all the experiments showed an aortic regurgitation (i.e., Exp. 3). This would lead to the assumption that aortic regurgitation is strictly dependent on catheter position, but the amount of experimental data does not permit this hypothesis to be confirmed. For this reason, a relatively high value of Rinv was considered so that it would not overly affect the results of the comparison analysis between the PUCA pump and the IABP.

The results in Figure 4 show that the performance of both devices reduces as Els increases and IABP performance especially seems to be strongly influenced by this ventricular variable. For lower values of Els, the effects of the PUCA pump in terms of the increment in CO and CBF are similar to those of the IABP. The difference between the two devices becomes progressively more marked for higher values of Els. In this case, the PUCA pump seems to ensure an improvement in hemodynamic conditions as well, while the IABP assistance does not lead to an increment in CO or CBF. P2 simulations were conducted in order to understand if a higher PUCA pump flow could assure a better hemodynamic effect. Results show that P2 ensures a higher effect in comparison to P1 in terms of both hemodynamic and energetic variables.

In the second step of the comparison, attention was focused on the influence of Csa on both devices. For this purpose similar experiments were conducted taking into account a lower value of Csa (I2, P3, P4, and P5 in Fig. 5). In this case, the performance of both devices was significantly improved. The IABP pump especially showed a high sensitivity to the stiffness of the system, making the hemodynamic results of I2 better than both P3 and P4. This gap is attenuated for energetic variables, so that DPTI and EVR changes are comparable for both P3 and I2. Under these new hemodynamic conditions an additional experiment was conducted for the PUCA pump by considering a catheter diameter of 25 Fr providing a flow of 5 l/min. Results show an improvement in PUCA pump effects in terms of CO, CBF, DPTI, and EVR, making its performance remarkably better than that of the IABP. In general, both energetic and hemodynamic results show that the PUCA pump offers a better performance as the PUCA pump flow is progressively increased (3.0 l min^{-1} for P3, 3.7 l min^{-1} for P4, and 5 l min^{-1} for P5). This permits results comparable to those of the IABP to be obtained for a stiffer cardiovascular system as well.

From Figures 4 and 5 it is evident how different the effects of a change in Csa are on the two devices. Probably in the case of a stiffer cardiovascular system, the presence of aortic regurgitation plays a role in redistributing blood flows in coronary and systemic circulations, thus appreciably affecting hemodynamic results.

In addition, from energetic point of view it must be said that in the case of the PUCA pump, the simulation of an aortic regurgitation caused a change in the morphology of Plv and Pas waveforms in the diastolic phase: the mean diastolic Plv increases and the mean diastolic Pas decreases. This contributes to reducing the difference between Pas and Plv used in Eq. (10) to calculate DPTI, especially for severe aortic regurgitation it is particularly important that these equations be used. To verify this hypothesis, a Rinv of 325 g·cm^{-4} s^{-1} was considered, according to Exp. 2 (Tab. IV). For these new hemodynamic conditions, the values of DPTI before and after PUCA pump activation were calculated. It was found that for Csa = 3.3 cm^3 $mmHg^{-1}$ and Csa = 1 cm^3 $mmHg^{-1}$, DPTI is about one half and one-third of the DPTI obtained under the same hemodynamic conditions but without aortic regurgitation, respectively.

In a previous work, the oxygen supply was evaluated using the diastolic time index (DTI) calculated as follows (3):

$$DTI = \int_{diastole} P_{ao}\,dt \times HR \qquad \text{(Eq.) (12)}$$

where P_{ao} is the pressure in the ascending aorta.

Using Eq. (12), DTI values obtained for both devices (PUCA pump with aortic regurgitation and IABP without aortic regurgitation) are closer, so that it was possible to compare percentage variations relative to both devices. But on the other hand, Eq. (12) does not take into account that the driving force generated by the ventricle is partly related to the difference between Plv and Pas (27). Besides, if we compare Eqs. (10) and (12) without considering HR and with the approximation Pas= P_{ao} it is possible to write:

$$DPTI = \int_{diastole} (Pas - Plv)dt = \int_{diastole} Pas \times dt - \int_{diastole} Plv \times dt = DTI - \int_{diastole} Plv \times dt \qquad \text{(Eq.) (13)}$$

Considering the variation of DPTI before and after PUCA pump activation it is possible to write:

$$\Delta DPTI = DPTI_2 - DPTI_1 = \Delta DTI + \int_{diastole} (Plv_1 - Plv_2) \times dt \quad \text{(Eq.) (14)}$$

where subscripts 1 and 2 refer to data before and after PUCA pump activation, respectively.

As the PUCA pump contributes to unload the ventricle and, as a consequence, to decrease the diastolic left ventricular pressure (5), the difference between Plv_1 and Plv_2 will assume positive values. From one point of view, the use of DTI permits comparable values for both the PUCA pump and the IABP to be obtained. But on the other hand, DTI may lead to underestimating the increment in oxygen availability due to the counterpulsation effects.

As pointed out earlier, this analysis takes into account the short-term effects of both devices on hemodynamics and energetics. Some comments on this methodology are necessary. The choice to take into account short-term effects of assistance corresponds to the idea that mechanical assistance, in the forms of both the PUCA pump and the IABP, should create the conditions for the onset of a virtuous circle leading to the recovery of the failing ventricle. The evolution of the ventricular conditions from this "starting point" and the outcome of the assistance depend on several factors (such as the primary cardiomyopathy process, the timing when the assistance is initiated, medical therapy, assist device weaning protocol (28)) and are hardly predictable using this modeling tool.

The whole circulatory model was used without any autonomic features as the aim of the study was to analyze and compare the short-term effects of the PUCA pump and the IABP and their sensitivity to specific circulatory and ventricular parameters. For this reason, the absence of autonomic controls in the circulatory model, and especially in the coronary circulation model, is not critical as the comparison between devices is possible in any case. This remark does not exclude of course the need to develop the model including autonomic controls among its features.

Another remark concerns the use of variables such as DPTI and EVR to analyze energetics of the assistance. Ventricular energetics could certainly be better analyzed using variables as external work, pressure-volume area, and cardiac mechanical efficiency. On the other hand, these variables are not easily measurable and are not universally used in clinics. It should also be taken into account that IABP performance analysis is traditionally based on DPTI and EVR, directly describing the balloon action. In spite of their limitations, ror these reasons it was decided to use DPTI and EVR for energetic analysis.

The last remark concerns the number of animals used, which precludes the possibility of any statistical analysis. It must be said that the aim of this work was not to validate the numerical model of the IABP or the PUCA pump, as this has already been done in previous works (1, 2, 5, 18). For this reason, experimental data were used with the main purpose of reproducing the possible working conditions of a left ventricle in the presence of a PUCA pump.

CONCLUSIONS

The numerical models of both the PUCA pump and the IABP make it possible to reproduce *in vivo* experiments and literature data with good accuracy so that they can be used to assess the performance of both devices under different working conditions. Numerical experiments show that both IABP and PUCA pump efficacy strongly diminishes with improved hemodynamic conditions (increase in Csa and Els). In the case of the PUCA pump, good performance is ensured in all cases both in terms of the increment in CO and CBF and in terms of the increment in DPTI and EVR . The IABP performance is strongly reduced for higher values of Els and Csa and in some cases the effect of IABP is the opposite of what might be expected: CBF does not increase and CO actually drops. But on the other hand, for lower values of Csa the performance of the IABP strongly improves in comparison to the PUCA pump. Further studies should be conducted to assess the hemodynamic and energetic effects of both pump systems on the simulated cardiovascular system by also taking into account the different pump synchronization ratios. To perform an analysis going beyond the short-term effects of both devices, the transformation of the model into what is called a virtual patient should be started, taking into account the autonomic response of the cardiovascular system and the autoregulation phenomena of coronary vasculature.

A preliminary, important general conclusion can in any case be drawn on the basis of the performed comparison. The choice of one device or the other is not univocal but depends on several factors, including important circulatory and ventricular parameters. Both the type and the control strategy of the assistance should therefore be "tailored" to

the single patient, by analyzing his or her initial circulatory conditions and evaluating first of all ventricular end systolic elastance and systemic arterial compliance. Finally, it is worth remarking that an important feature of the PUCA pump is its flexibility, enabling its performance to be modulated in relation to clinical needs, something that is not possible with the IABP.

Conflict of interest statement: Authors have no conflict of interest to declare.

Address for correspondence:
Ing. Libera Fresiello
Istituto di Fisiologia Clinica CNR
Sezione di Roma - Gruppo di Ingegneria Cardiovascolare
Via San Martino della Battaglia, 44
00148 Roma, Italy
e-mail: libera.fresiello@gmail.com

REFERENCES

1. Verkerke GJ, Mihaylov D, Geertsema AA, Lubbers J, Rakhorst G. Numerical Simulation of the Pulsating Catheter Pump: A Left Ventricular Assist Device. Artif Organs. 1999;23(10):924-931. Medline doi:10.1046/j.1525-1594.1999.06249.x
2. Jaron D, Moore TW, He P. Theoretical considerations regarding the optimization of cardiac assistance by Intra-aortic balloon pumping. IEEE Trans Biomed Eng. 1983;BME-30(3):177-186. doi:10.1109/TBME.1983.325106
3. Vandenberghe S, Segers P, Josemans H, Van Loon JP, Rakhorst G, Verdonck P. In vitro assessment of the unloading and perfusion capacities of the PUCA II and the IABP. Perfusion. 2004;19:25-32. Medline doi:10.1191/0267659104pf710oa
4. Mihaylov D, Verkerke GJ, Blanksma PK, Elstrodt J, De Jong ED, Rakhorst G. Evaluation of the optimal driving mode during left ventricular assist with pulsatile catheter pump in calves. Artif Organs. 1999;23(12):1117-1122. Medline doi:10.1046/j.1525-1594.1999.06307.x
5. Verkerke GJ, Geertsema AA, Mihaylov D, Blanksma PK, Rakhorst G. Numerical simulation of the influence of a left ventricular assist device on the cardiovascular system. Int J Artif Organs. 2000;23(11):765-773.
6. Bolooki H. Pulsatile Assist Device and Counterpulsation. In: Bolooki H. Clinical application of intra-aortic balloon pump. Mount Kisco, NY: Futura Pub Co Press; 1984: 13-18.
7. Dagan J. Pulsatile mechanical and mathematical model of the cardiovascular system. Med Biol Eng Comput. 1982;20(5):601-607. Medline doi:10.1007/BF02443408
8. Zhou J, Armstrong GP, Medvedev AL, Smith WA, Golding LA, Thomas JD. Numeric modeling of the cardiovascular system with a left ventricular assist device. ASAIO J. 1999;45(1):83-89. Medline. doi:10.1097/00002480-199901000-00019
9. Geertsema AA, Rakhorst G, Mihaylov D, Blanksma PK, Verkerke GJ. Development of a numerical simulation model of the cardiovascular system. Artif Organs. 1997;21(12):1297-1301. Medline. doi:10.1111/j.1525-1594.1997.tb00492.x
10. Heldt T, Shim EB, Kamm RD, Mark RG. Computational modeling of cardiovascular response to orthostatic stress. J Appl Physiol. 2002;92(3):1239-1254.
11. Ferrari G, De Lazzari C, Di Molfetta A, Fresiello L. Comprehensive Cardiovascular Modelling: Cardiovascular And Respiratory Systems. In: Darowski M, Ferrari G, eds. Comprehensive Models of Cardiovascular and Respiratory Systems: Their Mechanical Support and Interactions. New York, NY: Nova Science Publishers Inc.; 2010: 39-73.
12. Ferrari G, De Lazzari C, Mimmo R, Tosti G, Ambrosi D. A modular numerical model of the cardiovascular system for studying and training in the field of cardiovascular physiopathology. J Biomed Eng. 1992;14(2):91-107. Medline doi:10.1016/0141-5425(92)90014-C
13. Gilbert JC, Glantz SA. Determinants of left ventricular filling and of the diastolic pressure-volume relation. Circ Res. 1989;64:827-852.
14. Sagawa K, Maughan L, Suga H, Sunagawa K. Chamber Pressure-Volume Relation Versus Muscle Tension-Length Relaxation. In: Sagawa K, Maughan L, Suga H, Sunagawa K, eds. Cardiac Contraction and the Pressure-Volume Relationship. New York, NY: Oxford University Press; 1988:61-94.
15. Mantero S, Pietrabissa R, Fumero R. The coronary bed and its role in the cardiovascular system: a review and an introductory single-branch model. J Biomed Eng. 1992;14(2):109-116. Medline doi:10.1016/0141-5425(92)90015-D
16. De Lazzari C. A pumping heart coupled to lumped description of the cardiovascular compartments (CARDIOSIM©). In: De Lazzari C. Modelling Cardiovascular System and Mechanical Circulatory Support. Rome: CNR (Roma); 2007:65-67.

17. Fresiello L, De Lazzari C, Trivella MG, Di Molfetta A, Ferrari G. Influence of the pulsatile catheter pump synchronization on haemodinamic variables: numerical simulation. Proceedings of the 7th IASTED International Conference Biomedical Engineering. BioMED 2010.
18. Jaron D, Moore TW, He P. Control of Intraaortic balloon pumping: theory and guidelines for clinical applications. Ann Biomed Eng. 1985;13:155-175. Medline doi:10.1007/BF02584236
19. Trivella MG, De Lazzari C. Mechanical circulatory support system (MCSS) In: De Lazzari C. Modelling Cardiovascular System and Mechanical Circulatory Support. Rome: CNR (Roma); 2007:174-177.
20. Darowski M, De Lazzari C, Ferrari G, Clemente F, Guaragno M. The influence of simultaneous intra-aortic balloon pumping and mechanical ventilation on hemodynamic parameters-numerical simulation. Front Med Biol Eng. 1999;9(2):155-174.
21. Burattini R, Gnudi G, Westerhof N, Fioretti S. Total Systemic Arterial Compliance and Aortic Characteristic Impedance in the Dog as a Function of Pressure: A Model Based Study. Comput Biomed Res. 1987;20(2):154-165. Medline doi:10.1016/0010-4809(87)90042-5
22. Schreuder JJ, Maisano F, Donelli A, et al. Beat-to-Beat Effects of Intraaortic Balloon Pump Timing on Left Ventricular Performance in Patients With Low Ejection Fraction. Ann Thorac Surg. 2005;79:872-880. Medline. doi:10.1016/j.athoracsur.2004.07.073
23. Kawaguchi O, Pae WE, Daily BB, Pierce WS. Ventriculoarterial coupling with intra-aortic balloon pump in acute ischemic heart failure. J Thorac Cardiovasc Surg. 1999;117:164-171. Medline. doi:10.1016/S0022-5223(99)70482-4
24. Papaioannou TG, Mathioulakis DS, Stamatelopoulos KS, et al. New aspects on the role of blood pressure and arterial stiffness in mechanical assistance by intra-aortic balloon pump: in-vitro data and their application in clinical practice. Artif Organs. 2004;28(8):717-727. Medline doi:10.1111/j.1525-1594.2004.00080.x
25. Ferrari G, Górczyńska K, Mimmo R, et al. IABP assistance: a test bench for the analysis of its effects on ventricular energetics and hemodynamics. Int J Artif Organs. 2001;24(5):274-280.
26. Bolooki H. Physiology of Balloon Pumping. In: Bolooki H. Clinical application of intra-aortic balloon pump. Mount Kisco, NY: Futura Pub Co Press; 1984: 115-119.
27. Reitan JA, Martucci RW, Levine NA. A computer evaluation of the ratio of the diastolic pressure-time index to the time-tension index from three arterial sites in dogs. J Clin Monit. 1986;2:95-99. Medline doi:10.1007/BF01637675
28. Kumpati GS, McCarthy PM, Hoercher KJ. Left Ventricular Assist Device Bridge to Recovery: A Review of the Current Status. Ann Thorac Surg. 2001;71:S103-108. Medline. doi:10.1016/S0003-4975(00)02630-8.